Molecular Crystals and Liquid Crystals Science and Technology. Section A. Molecular Crystals and Liquid Crystals
Publication details, including instructions for authors and subscription information:
http://www.tandfonline.com/loi/gmcl19

Modeling Internal Chain Dynamics in Nematogens of Different Chain Lengths: Deuteron NMR Study

Ronald Y. Dong [a b] & G. M. Richards [a]

[a] Department of Physics and Astronomy, Brandon University, Brandon, Manitoba, R7A 6A9

[b] Physics Department, University of Manitoba, Winnipeg, Manitoba, R3T 2N2

Version of record first published: 23 Sep 2006.

To cite this article: Ronald Y. Dong & G. M. Richards (1995): Modeling Internal Chain Dynamics in Nematogens of Different Chain Lengths: Deuteron NMR Study, Molecular Crystals and Liquid Crystals Science and Technology. Section A. Molecular Crystals and Liquid Crystals, 262:1, 339-355

To link to this article: http://dx.doi.org/10.1080/10587259508033537

Mol. Cryst. Liq. Cryst. 1995, Vol. 262, pp. 339–355
Reprints available directly from the publisher
Photocopying permitted by license only

MODELING INTERNAL CHAIN DYNAMICS IN NEMATOGENS OF DIFFERENT CHAIN LENGTHS: DEUTERON NMR STUDY

RONALD Y. DONG[†,*] and G. M. Richards[†]
[†]Department of Physics and Astronomy, Brandon University, Brandon, Manitoba R7A 6A9
[*]Physics Department, University of Manitoba, Winnipeg, Manitoba R3T 2N2

Abstract Aligned liquid crystals with deuterated chains show well-resolved deuterium NMR spectra. The site specificity of these quadrupolar doublet signals allows measurements of both static and dynamic observables, which can provide information on the rotation dynamics within the flexible end chain. We use a realistic geometry and the rotational isomeric model of Flory to generate all possible configurations and a set of C-D bond orientations in the chain. A master rate equation is used to describe transitions among all allowed configurations of the chain. In this paper, we report on motional parameters derived from quantitative fittings of quadrupolar splitting and spectral density data in three different nematogens of various chain lengths. The deuterated samples are p-methoxy-d_3-benzylidene-d_1-p-n-butyl-d_9-aniline (1O.4-d_{13}), 4-n-pentyl-d_{11}-4′-cyanobiphenyl-d_4 (5CB-d_{15}) and 4-n-hexyloxy-d_{13}-4′-cyanobiphenyl-d_8 (6OCB-d_{21}).

INTRODUCTION

The Southampton group[1,2] was first to use deuterium spin relaxation techniques to study 4-n-pentyl-d_{11}-4′-cyanobiphenyl-d_4 (5CB-d_{15}) and was able to examine in detail the internal and overall motions of this nematogen. Recently, many workers[3] have chosen this approach to study molecular dynamics of liquid crystals. The advantages are 1. the deuterium NMR spectra show well-resolved quadrupolar doublets associated with the various atomic sites in the molecule and 2. multi-pulse NMR techniques may be applied to give a direct measure of spectral densities at these sites. The 5CB molecule has a flexible pentyl chain. Beckmann et al.[2] used a superimposed rotations model in which diffusive rotations about various

carbon-carbon (C-C) bonds in the chain were assumed to be independent of each other and could be superimposed onto the overall motion of the molecule. Later concerted internal rotations in the pentyl chain were tackled by us[4] and Ferrarini et al.[5] using the master equation method. The approach[6] used for concerted internal dynamics of macromolecules dissolved in solutions was extended to liquid crystals[4]. It represented a time-domain extension of the rotational isomeric state (RIS) model of Flory[7]. For simplicity, our model assumed that internal rotations can be decoupled from the overall reorientation of the molecule and that a diamond (tetrahedral) lattice can be used to describe conformations of the C-C backbone in the chain. This decoupled model was applied to 5CB[4,5,8] with the equilibrium probabilities for various conformations calculated according to the nematic mean-field potential. The overall motion of the molecule has been described by a small-step rotational diffusion model proposed by Nordio et al.[9,10]. Since the diamond lattice was found to fail in modeling the quadrupolar splittings in liquid crystals[11,12], we have adopted a realistic geometry instead of the diamond lattice in our recent studies of p-methoxy-d_3-benzylidene-d_1-p-n-butyl-d_9-aniline (1O.4-d_{13})[13] and 4-n-hexyloxy-d_{13}-4′-cyanobiphenyl-d_8 (6OCB-d_{21})[14] using the decoupled model.

In this paper, we present new experimental data for 5CB-d_{15} at 46 MHz, but note that limited data at this frequency were given[8] before. We use here the same refinement as in 1O.4 and 6OCB to fit the experimental and calculated spectral densities of 5CB. For 1O.4 and 5CB, we also examine the applicability of the 'third rate' model[15] and compare it with Nordio's model. We note that the third rate model has been found to be superior in describing spin relaxation due to the overall motion in 1O.4[13] and in 4-n-pentyloxybenzylidene-4′-heptylaniline (5O.7)[16]. As in previous studies[2,8], the contribution from director fluctuations[17,18] is assumed to be small for deuterium spin relaxation in the MHz region and can be neglected. Thus far, we found only 5O.7[16] in which this assumption is unwarranted in the MHz region. In the following section, a brief description of the experimental method is given. The next section presents interpretation of the results. A computer program[8] is used to separately fit the quadrupolar splittings and spectral densities

by using a minimization routine AMOEBA[19]. The last section contains a brief summary and conclusions of this work.

EXPERIMENTAL

The 10.4-d_{13}, 5CB-d_{15} and 6OCB-d_{21} samples were purchased from Merck, Sharp and Dohme Canada and used without further purification. The sample temperature of 5CB was calibrated using the reported quadrupolar splittings[11] of the Southampton group who used a clearing temperature (T_c) of 35.3°C. The 6OCB-d_{21} sample has a T_c of 75°C, while the 10.4-d_{13} has a T_c of 39.5°C. Broadband Jeener-Broekaert (J-B) sequence or the simple J-B sequence with the appropriate phase-cycling of radiofrequency and receiver phases[3] was used to simultaneously measure the Zeeman (T_{1Z}) and quadrupolar (T_{1Q}) spin-lattice relaxation times. Signal collection was started ca. 10 μs after each monitoring $\pi/4$ pulse. For 5CB, signal was averaged up to 1600 scans at 15.3 MHz and over 32-96 scans at 46 MHz. The experimental setup and procedures for data reduction have been described elsewhere[13,20]. The experimental uncertainty in the spin-lattice relaxation times was estimated to be ±5% or better. Since the T_{1Z} and T_{1Q} are given[3] for spin I=1 by the standard spin relaxation theory

$$\begin{aligned} T_{1Z}^{-1} &= J_1(\omega_0) + 4J_2(2\omega_0) \\ T_{1Q}^{-1} &= 3J_1(\omega_0)\,, \end{aligned} \tag{1}$$

they can be used to separate the two spectral densities of motion $J_1(\omega_0)$ and $J_2(2\omega_0)$ at the Larmor frequency $\omega_0/2\pi$ and twice the Larmor frequency, respectively.

RESULTS AND INTERPRETATION

The spectral densities of 5CB-d_{15} at 15.3 and 46 MHz are presented as a function of temperature in figure 1. The spectral density data of 10.4-d_{13} and 6OCB-d_{21} and the theory of the decoupled model with modifications to account for a realistic geometry in the chain have been described elsewhere[13,14]. Expressions of spectral densities will only be given here to aid the discussion. The reader

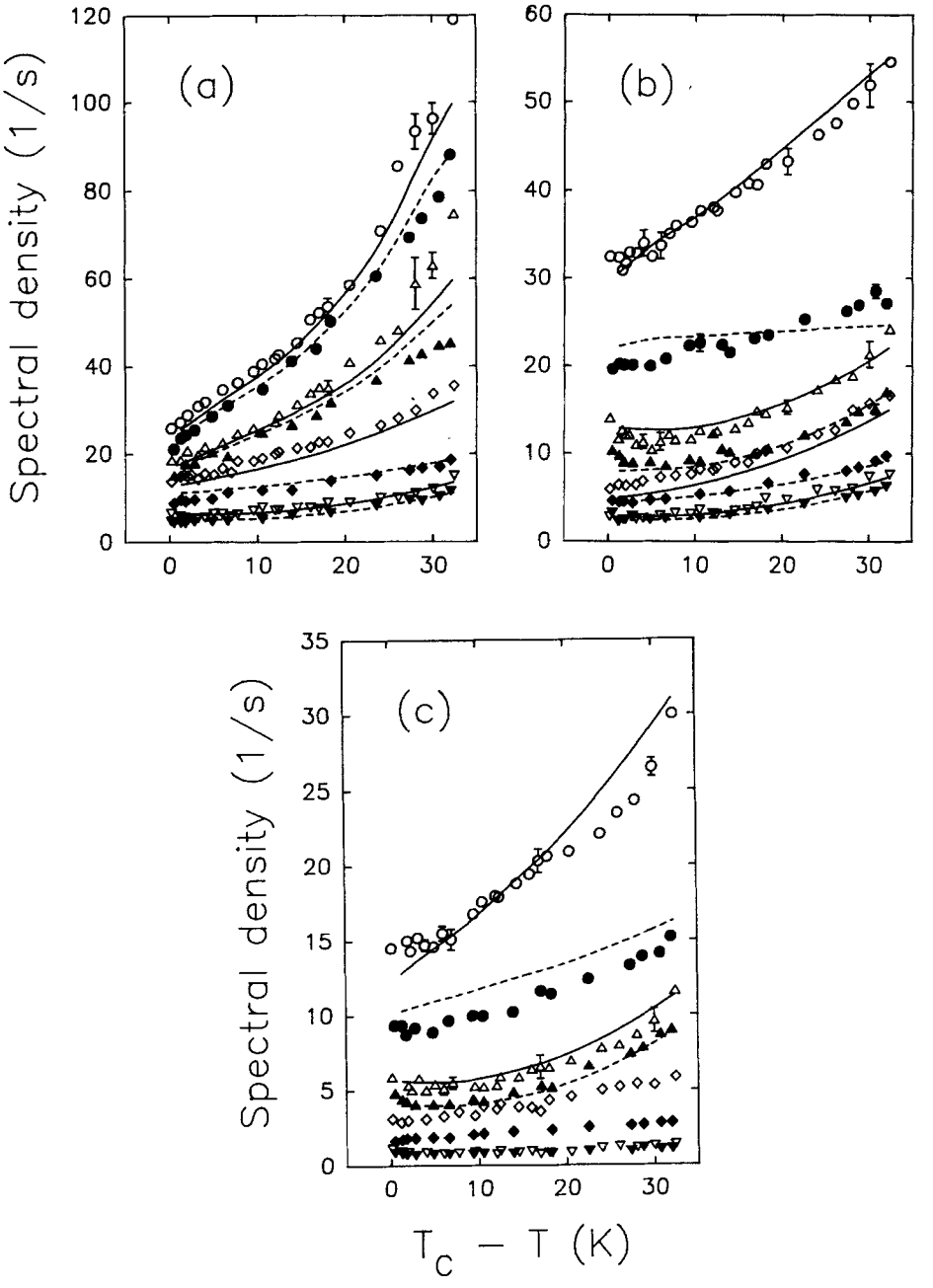

FIGURE 1 Plots of spectral densities versus $T_c - T$ in 5CB-d_{15}. Open and closed symbols denote 15.3 MHz and 46 MHz data, respectively. ○ and △ denote $J_1^{(i)}(\omega)$ and $J_2^{(i)}(2\omega)$, while ◇ and ▽ denote $J_1^{(j)}(\omega)$ and $J_2^{(j)}(2\omega)$, respectively. (a) i = ring and j = C_2, (b) i = C_1 and j = C_4, and (c) i = C_3 and j = C_5. Solid and dashed curves are theoretical predictions based on Nordio's model for 15.3 and 46 MHz, respectively.

is therefore asked to refer to our previous papers for detail. In all nematogens, we model the experimental data in a self consistent manner by first fitting the quadrupolar splittings and using the derived interaction parameters (X_a for the core that includes the C_{ar}-C_1 or the C_{ar}-O bond and X_{cc} for a C-C bond) and $< P_2 >$, the order parameter of an 'average' conformer in subsequent fitting of the spectral densities. At each chosen temperature, we fit the quadrupolar splittings by minimizing the sum squared error f,

$$f = \sum_i \left[S_{CD}^{(i)}(expt) - S_{CD}^{(i)}(calc)\right]^2 \tag{2}$$

and the spectral density data by minimizing the sum squared percentage error F,

$$F = \sum_\omega \sum_i \sum_{m_L} \left[\frac{J_{m_L}^{(i)}(m_L\omega)_{expt} - J_{m_L}^{(i)}(m_L\omega)_{calc}}{J_{m_L}^{(i)}(m_L\omega)_{expt}} \times 100\right]^2 \tag{3}$$

The fitting quality factor Q in the spectral density calculations is given by the percentage mean-squared deviation

$$Q = \frac{\sum_\omega \sum_i \sum_{m_L} \left[J_{m_L}^{(i)}(m_L\omega)_{expt} - J_{m_L}^{(i)}(m_L\omega)_{calc}\right]^2}{\sum_\omega \sum_i \sum_{m_L} \left[J_{m_L}^{(i)}(m_L\omega)_{expt}\right]^2} \times 100 \tag{4}$$

The realistic geometry for the alkyl(oxy) chain was given[21] by $\angle$CCH = 107.5°, $\angle$HCH = 113.6°, $\angle$CCC = 113.5° and the dihedral angles ϕ = 0, ± 112° for the three RIS. The quadrupolar coupling constant (q_{CD}) was taken as 168 kHz for the methylene deuterons, and 185 kHz for the methine and ring deuterons. The C_{ar}-C_1 or C_{ar}-O bond was taken to be along the biphenyl *para* axis and the ring C-D bond made an angle of 60° with the *para* axis. We assumed the biphenyl core to be cylindrically symmetric[4]. In 6OCB, we treated[22] the O-C and C-O bonds like a C-C bond, except the $\angle$COC (= 126°) and their bond lengths are different. In 5CB and 6OCB, the sum over i for f included only the data from the methylene deuterons in the chain, while for F the ring data were also included in the sum, i.e. data from the methyl deuterons was not included in either minimization. Since 1O.4-d_{13} has a shorter chain and its results have been discussed[13], a brief summary is given first. The analyses of 5CB data then follow. Limited success[14] in fitting

the spectral density data of 6OCB-d_{21} was reported. Here we examine further the fitting of the available spectral densities over the entire nematic range of 6OCB.

p-Methoxybenzylidene-p-n-butylaniline

For the butyl chain of 1O.4, there are 27 configurations since the first dihedral angle in the chain (at the junction of the aniline ring) is allowed to sample three RIS. The allowed configurations are generated by the RIS model and the orientations of one set of chain C-D bonds in the molecular frame are obtained. The transition rate matrix $\underline{\underline{R}}$ that describes conformational changes in the chain is a 27×27 matrix and contains jump rate constants k_1, k_2 and k_3 for the one-, two- and three-bond motions in the chain. We found[13] that the overall motion of this nematogen can best be described by the third rate model. In this model, the rotational diffusion tensor of the molecule is chosen to be diagonal in the laboratory (director) frame with principal diffusion constants D_α and D_β. The D_α describes diffusion of the molecule around the director, while D_β describes diffusion about an axis perpendicular to the director. The third rate constant in the model is D_γ which accounts for fast rotation of the molecule about its long molecular axis. With this division of the molecular motion, the rotational correlation times are[15]

$$(\tau^{(j)}_{m_L m_M})^{-1} = h_{m_M} + \left[6D_\beta + m_L^2(D_\alpha - D_\beta)\right] / b^{(j)}_{m_L m_M} \tag{5}$$

where $h_0 = 0, h_1 = D_\gamma$ and $h_2 = (3p+1)D_\gamma$ with $0 \leq p \leq 1$ with $p = 0$ corresponding to strong collision and $p = 1$ to small step rotational diffusion. The $b^{(j)}_{m_L m_M}$ are defined below. To illustrate the model, we present in figure 2 the experimental and calculated spectral densities of 1O.4-d_{13} at two different temperatures. The derived motional parameters are given in table I.

TABLE I: Model parameters for 1O.4 derived from the third rate model. The diffusion constants and jump rates are in units of 10^9 s^{-1}.

T (K)	D_α	D_β	D_γ	k_1	k_2	k_3	p	Q
291	0.014	0.027	1.7	1.1×10^2	2.7×10	7.6×10^2	0.40	0.4 %
303	0.057	0.036	3.8	4.4×10^2	2.4×10	1.6×10^3	0.26	0.5 %

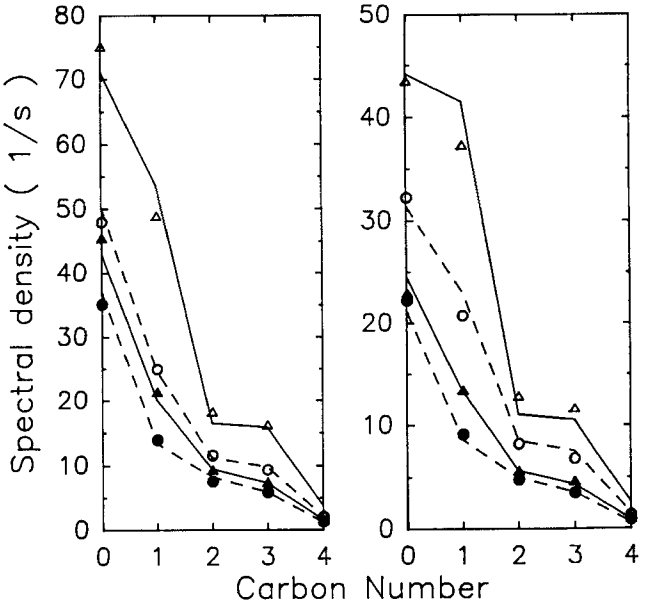

FIGURE 2 Plots of spectral densities versus the carbon number in 1O.4 at 291 (left) and 303K (right). Solid (15.3 MHz) and dashed (46 MHz) lines denote calculated spectral densities using the third rate model. Open and closed symbols denote $J_1(\omega)$ and $J_2(2\omega)$, respectively.

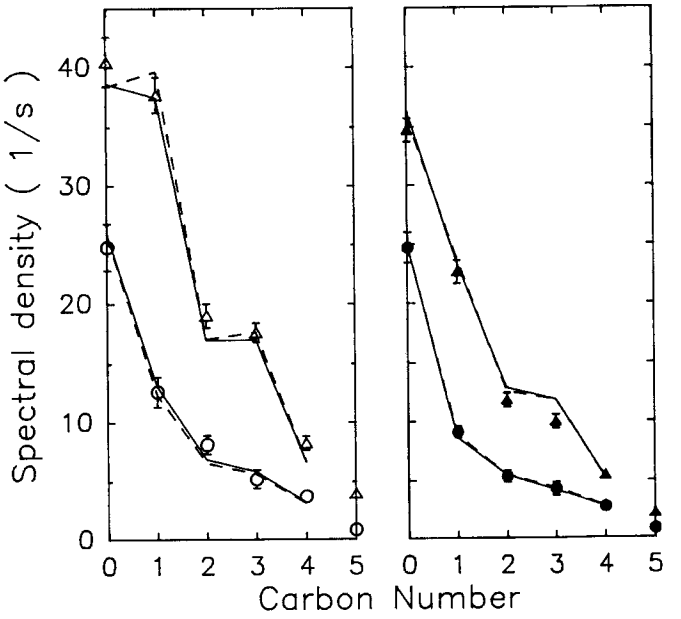

FIGURE 3 Plot of spectral densities $J_1(\omega)(\triangle)$ and $J_2(2\omega)(\bigcirc)$ in 5CB at 298K. Open andclosed symbols denote data at 15.3 and 46 MHz, respectively. Solid and dashed lines are calculated from Nordio's model and the third rate model, respectively.

4-n-Pentyl-4′-cyanobiphenyl

The number of configurations in the pentyl chain of 5CB is 81 since the first dihedral angle in the chain samples all three RIS. The $\underline{\underline{R}}$ matrix is now 81×81. In the decoupled model, the spectral densities $J^{(i)}_{m_L}(m_L\omega)$ of the C_i deuteron(s) for $m_L \neq 0$ are given by

$$J^{(i)}_{m_L}(m_L\omega) = \frac{3\pi^2}{2}(q^{(i)}_{CD})^2 \sum_{m_M}\sum_{n=1}^{81} c_{m_L m_M} \left|\sum_{l=1}^{81} d^2_{m_M 0}(\beta^{(i)l}_{M,Q}) \exp\left[-im_M \alpha^{(i)l}_{M,Q}\right] x^{(1)}_l x^{(n)}_l\right|^2 \times \sum_j a^{(j)}_{m_L m_M}\left[(\tau^{(j)}_{m_L m_M})^{-1} + |\Lambda_n|\right] / \left\{(m_L\omega)^2 + \left[(\tau^{(j)}_{m_L m_M})^{-1} + |\Lambda_n|\right]^2\right\} \quad (6)$$

where $\beta^{(i)l}_{M,Q}$ and $\alpha^{(i)l}_{M,Q}$ are the polar angles of the C_i-D bond of the l^{th} conformer in the molecular M frame (the z_M axis is along the ring *para* axis). $a^{(j)}_{m_L m_M}$ and $b^{(j)}_{m_L m_M}$ represent, respectively, normalized relative weights and decay time constants in multi-exponentials of the correlation functions from which the spectral densities are obtained by Fourier transforming, and $c_{m_L m_M}$ are the mean squares of the Wigner rotation matrices. The a, b and c coefficients depend on the order parameter $< P_2 >$ and are tabulated[15] for a Maier-Saupe potential. The rotational correlation times $\tau^{(j)}_{m_L m_M}$ are given in Nordio's model[9,10] by

$$(\tau^{(j)}_{m_L m_M})^{-1} = [6D_\perp + m^2_M(D_\parallel - D_\perp)]/b^{(j)}_{m_L m_M} \quad (7)$$

with $D_\parallel$ and $D_\perp$ being the rotational diffusion constants of an 'average' conformer about its z_M axis and about an axis normal to the z_M axis. Λ_n and $\underline{x}^{(n)}$ are the eigenvalues and eigenvectors from diagonalizing a symmetrized $\underline{\underline{R}}$.

Assuming free internal ring rotation about its *para* axis with a diffusion constant D_R, the spectral densities for the ring deuterons are given by the superimposed rotations model[2]

$$J^{(R)}_{m_L}(m_L\omega) = \frac{3\pi^2}{2}(q^{(R)}_{CD})^2 \sum_{m_M}\sum_{m_R} c_{m_L m_M}\left[d^2_{m_R 0}(\beta_{R,Q})\right]^2\left[d^2_{m_M m_R}(\beta_{M,R})\right]^2 \times \sum_j a^{(j)}_{m_L m_M}\left[(\tau^{(j)}_{m_L m_M})^{-1} + (1-\delta_{m_R 0})D_R\right] / \left\{(m_L\omega)^2 + \left[(\tau^{(j)}_{m_L m_M})^{-1} + (1-\delta_{m_R 0})D_R\right]^2\right\} \quad (8)$$

where $\beta_{M,R}$ is the angle between the *para* axis and the z_M axis, and the internal ring rotation is assumed to be in the strong collision limit. Since $\beta_{M,R}$=0, it is hard to distinguish D_R from $D_{||}$ unless $\tau^{(j)}_{m_L m_M}$ can be determined from deuterated sites beside the ring. When the third rate model is used, the spectral densities are still given by eqs. (6) and (8) except that the $\tau^{(j)}_{m_L m_M}$ are given by eq. (5).

Both Nordio's model and the third rate model were used to model the experimental spectral densities from the ring deuterons and the deuterons attached to the first four carbons in the pentyl chain. We note that three model parameters (D_α, D_β and D_γ) are used to describe overall motion in the third rate model, while there are only two model parameters ($D_\perp$ and $D_{||}$) in Nordio's model. The parameters derived from the order parameter profile analysis were used in these calculations, namely $\beta_{R,Q} = 60°$, $E_{tg} = 3.8$ kJ/mol, $E_{g^\pm g^\mp} = 0$ kJ/mol[21] and X_a, λ_x and $< P_2 >$ as listed in table II. Unlike 1O.4, both Nordio's model and the third rate model yield similar fits to the experimental spectral densities. We found that for both models, good fits can be achieved by varying k_1 and k_2 only and setting k_3 equal to $100k_2$. k_3 was not as well-defined as k_1 or k_2 and this assumption gave only a slight increase in F.

TABLE II: Interaction parameters and order parameters of the 'average' conformer derived from optimization of fits to experimental quadrupolar splittings of 5CB. $\lambda_x = X_{cc}/X_a$.

T (K)	X_a (kJ/mol)	λ_x	$< P_2 >$	$< S_{xx} >$ - $< S_{yy} >$
276.3	5.807	0.1443	0.647	0.0047
279.3	5.649	0.1460	0.632	0.0049
283.3	5.442	0.1482	0.611	0.0051
287.3	5.229	0.1505	0.589	0.0052
291.3	4.999	0.1528	0.565	0.0054
295.3	4.755	0.1550	0.538	0.0056
299.3	4.458	0.1574	0.505	0.0057
303.3	4.035	0.1602	0.458	0.0059
307.3	3.174	0.1644	0.362	0.0058

The results of Nordio's model are presented first. The fit between experimental and calculated spectral densities was good with F varying between 870 and 2500; the best fits were in the middle of the temperature range due to smoothed lines being used for the data. These errors translate into Q values of 0.2 - 1% (see table III), which compare favourably with our previously reported[8] values using a diamond lattice for the chain (0.1-1.9%), especially when we consider that in the present study the interaction parameters were derived directly from the splittings and that relaxation data from both frequencies were modeled simultaneously. The calculated temperature dependences for the spectral densities based on Nordio's model are given in figure 1. These plots show that the agreement between calculated and experimental values was generally very good, as would be expected from the low F values. Those deviations that did occur are mostly within the bounds of experimental error as indicated by the error bars. The experimental and predicted site dependences of the spectral densities at 298K are shown in figure 3. On close examination of figures 1 and 3, several small systematic errors are evident.

The temperature dependences of the three rotational diffusion constants are plotted in figure 4(a). With the exception of some pre-transitional behaviour $D_\perp$, $D_\parallel$ and D_R all show Arrhenius relationships with temperature; the activation energies (E_a) being similar, 26 ± 21, 33 ± 20 and 25 ± 18 kJ/mol, respectively. The E_a value for $D_\perp$ is small compared with the value of 54 kJ/mol obtained from dielectric relaxation[23]. This reflects the difficulty in getting information about tumbling motions of the molecule, i.e. large uncertainty in the E_a value of $D_\perp$. Over most of the temperature range $D_\parallel$ is approximately $20 \times D_\perp$, and $D_R/D_\parallel \simeq 2$. The calculated $D_\parallel$ and D_R values are very similar to those obtained in a previous study[8] using a diamond lattice for the chain when an E_a of 54 kJ/mol was assumed for $D_\perp$. The k_2 (and k_3) increases with temperature showing an Arrhenius relationship with an activation energy of 60.9 kJ/mol. k_1 decreases gradually with increasing temperature over most of the range, being roughly constant at the lowest temperatures. The k_1 and k_2 values are summarized in table III. We found that it is necessary to include all three jump rates in the model, since using a single rate constant, k,

would result in an unacceptable sixfold increase in F.

In the analysis of the spectral density data using the third rate model, we found that the parameter p that describes the γ-motion has a profound effect on the D_R value and on the D_γ/D_R ratio. The calculated values for D_γ and D_R for $p = 1.0$ showed expected temperature behaviours and were also close to $D_{||}$ and D_R obtained using Nordio's model. Therefore a p value of 1.0 was set for the final analysis of the spectral density data using the third rate model, which implies that the γ-motion is in the small step diffusive limit. The fits to the experimental spectral densities were good, as the F values varied between 850 and 2300. The predicted spectral densities for the third rate model at 298K are plotted in figure 3. This illustrates the few small differences between the predictions of the two models, which were consistent over the entire temperature range. The differences cancelled each other out in terms of error, as the F values for the two models were very similar. The temperature dependences of the three diffusion constants of the third rate model and D_R are plotted in figure 4(b). The error bars for the motional parameters in figure 4 were estimated by varying the parameter in question, while the others were set at those values from the minimization, to give a doubling in the F value. Over most of the temperature range D_α, D_β, D_γ and D_R all showed Arrhenius relationships with temperature, the activation energies being 26 ± 20, 23 ± 22, 31 ± 20 and 32 ± 17 kJ/mol, respectively. D_α is mostly slightly greater than D_β, except at low temperatures, and their values are comparable to the $D_\perp$ values of Nordio's model. We note that the uncertainty in the E_a for molecular tumbling (D_β) is again large, indicating that this motion is hard to determine. When compared with the rotational diffusion parameters derived for 1O.4 using the same model[13], D_α and D_β have similar values, and D_γ is $\sim$ three times slower for 5CB. The derived jump rates shown also in table III are very similar to those obtained using Nordio's model. The E_a for k_2 is 47.4 kJ/mol. It is interesting to note that the tumbling motion of molecules in mesophases, whether described by Nordio's model or the third rate model, is not only hard to quantify using the ring deuterons but even with the help of methylene deuterons in the chain.

TABLE III: Jump rate constants (in units of 10^9 s^{-1}) and Q-factor from optimization of fits to experimental spectral densities of 5CB. k_3 is set at $100k_2$.

	Nordio			Third Rate		
T (K)	k_1 (s^{-1})	k_2 (s^{-1})	Q (%)	k_1 (s^{-1})	k_2 (s^{-1})	Q (%)
276.3	3.0 x 10^2	3.1 x 10^2	1.0	3.6 x 10^2	2.6 x 10^2	0.9
279.3	3.2 x 10^2	3.7 x 10^2	0.8	3.7 x 10^2	3.2 x 10^2	0.8
283.3	3.3 x 10^2	4.8 x 10^2	0.4	3.8 x 10^2	4.2 x 10^2	0.5
287.3	3.3 x 10^2	6.6 x 10^2	0.2	3.8 x 10^2	5.5 x 10^2	0.3
291.3	3.0 x 10^2	9.5 x 10^2	0.2	3.6 x 10^2	7.6 x 10^2	0.2
295.3	2.6 x 10^2	1.4 x 10^3	0.2	3.4 x 10^2	1.0 x 10^3	0.3
299.3	2.2 x 10^2	1.9 x 10^3	0.3	3.0 x 10^2	1.3 x 10^3	0.4
303.3	1.8 x 10^2	2.5 x 10^3	0.5	2.8 x 10^2	1.4 x 10^3	0.6
307.3	1.0 x 10^2	5.0 x 10^3	0.7	1.6 x 10^2	2.2 x 10^3	0.7

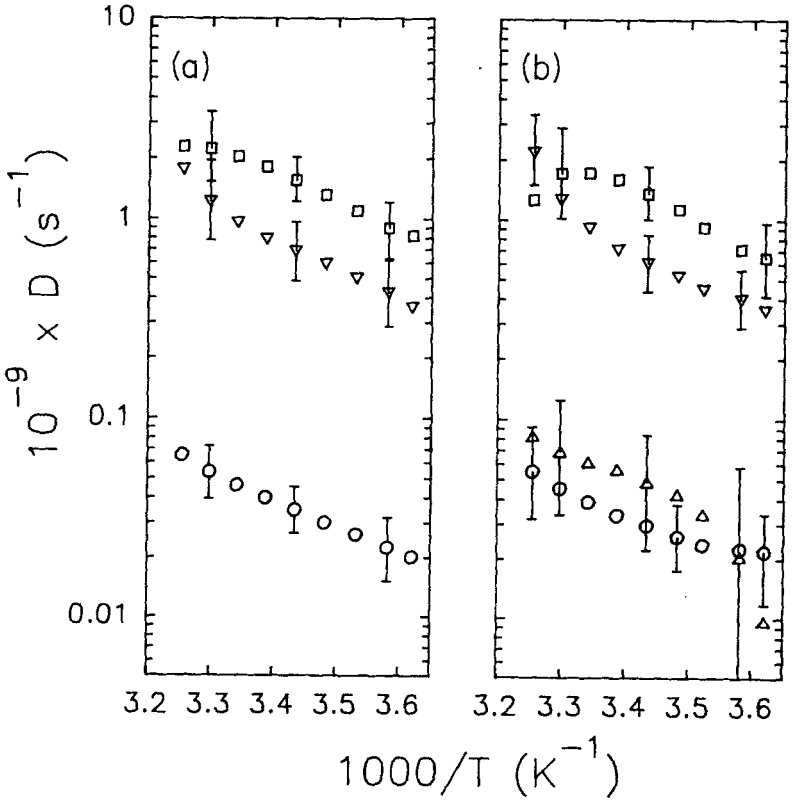

Figure 4 Plots of rotational diffusion constants versus the reciprocal temperature in 5CB. (a) Nordio's model: $D_{\|}$ (▽), D_R(□) and $D_{\perp}$(○), (b) Third rate model: D_{α}(△), D_{β} (○), D_{γ}(▽) and D_R(□).

4-n-Hexyloxy-4′-cyanobiphenyl

Preliminary spectral density data of 6OCB-d_{21} were recently given[14] together with our attempt to analyze these using the decoupled model. The overall motion was treated with Nordio's model. Although the quadrupolar splitting data were analyzed with 729 configurations (the O-C_1 bond sampled three RIS), the spectral density calculations that involved diagonalization of a 729×729 rate matrix and minimization with respect to the experimental values, were too time-consuming on a VAX workstation. Our analyses made use of the pentane effect to reduce the number of configurations to 297. The fits between experimental and calculated spectral densities[14] were acceptable ($Q < 3\%$) within 20° below T_c. It was found that the Q-factor increases with decreasing temperature and a large discrepancy exists in the fit of $J_2(2\omega)$ for C_1. To implement 729 configurations in the spectral density calculation, we used a faster DEC 3000 workstation and simplified the computer program using a θ angle between the ring *para* axis and the C_{ar}-O bond of 0° instead of the previous value[14] of 4°. We believe that the new θ angle would not significantly change the calculation. Now the minimization with 729 configurations would take about a day of CPU time. We have carried out these calculations over the entire nematic range, but the fits were marginally improved in comparison with those using the pentane effect. In particular, the difficulty with predicting $J_2(2\omega)$ for C_1 remains. We therefore, conclude that the dihedral angle (α_1) for the O-C_1 bond must be treated differently. Several possibilities[5] were tried. One of these is to place the O-C_1 bond at four equivalent sites, symmetrically placed with respect to both the aromatic ring and the plane perpendicular to it (i.e. $\pm\,\alpha_1$, $180° \pm\,\alpha_1$). We need to only consider configurations with either $\pm\,\alpha_1$ or $180° \pm\,\alpha_1$ due to the symmetry of the O-C_1 bond about a plane perpendicular to the aromatic ring. As a consequence, the $\underline{\underline{R}}$ matrix is 486×486. We have tried several different α_1 values and have chosen $\alpha_1 = 65°$ to do our calculations of the quadrupolar splittings and spectral densities. From the order parameter profile analysis of the methylene deuterons with $E_{tg} = 3.8$ kJ/mol, $E_{g^\pm g^\mp} = 0$ kJ/mol[22], we obtained X_a, λ_x and $< P_2 >$ as listed in table IV for the spectral density calculations. Again using

TABLE IV: Interaction parameters and order parameters of the 'average' conformer derived from optimization of fits to experimental quadrupolar splittings of 6OCB.

T (K)	X_a (kJ/mol)	λ_x	$< P_2 >$	$< S_{xx} > - < S_{yy} >$
311	7.67	0.1176	0.716	0.014
323	7.19	0.1169	0.677	0.014
335	6.16	0.1238	0.603	0.016
343	4.97	0.1311	0.505	0.018

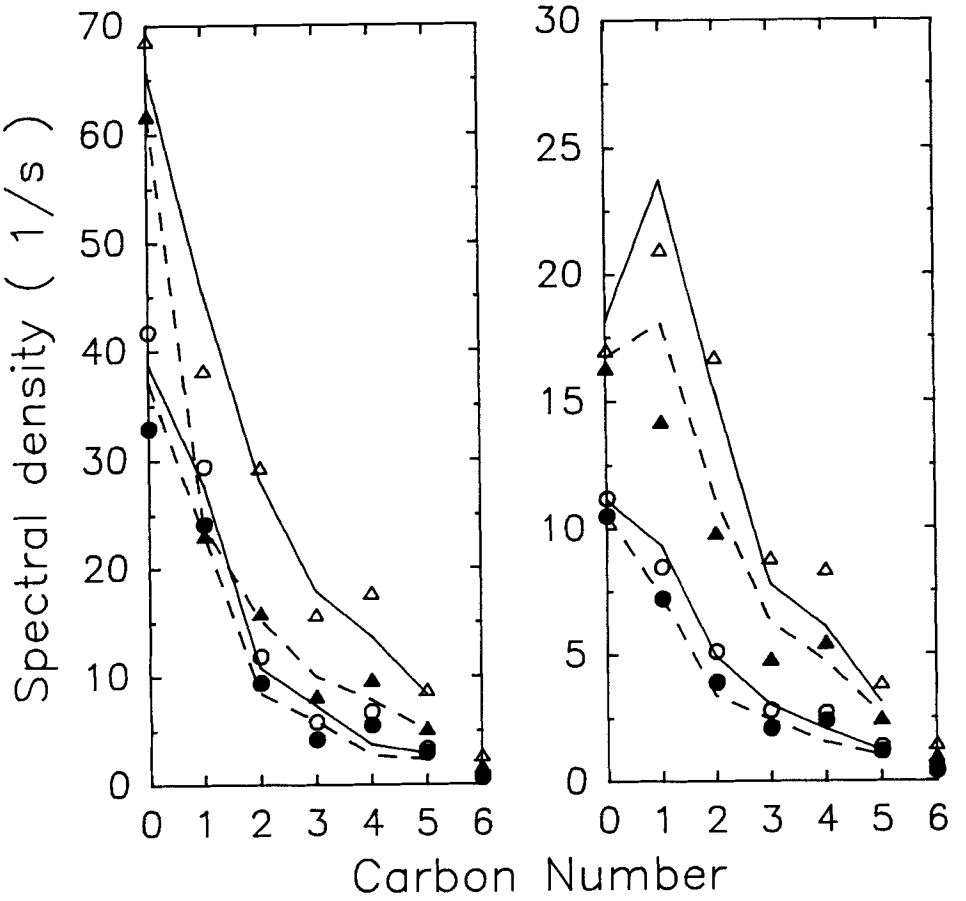

FIGURE 5 Plots of spectral densities $J_1(\omega)(\triangle)$ and $J_2(2\omega)(\bigcirc)$ versus the carbon number in 6OCB at 311 (left) and 343K (right). Carbon 0 refers to ring deuterons. Solid (15.3 MHz) and dashed (46 MHz) lines are calculated spectral densities based on model fitting. Open and closed symbols denote 15.3 and 46 MHz data, respectively.

eq. (7) in eqs. (6) and (8), the minimization between experimental and calculated spectral densities was carried out over the entire nematic range. We found that the fits were much improved at lower temperatures, but not so at high temperature. However, the fits of $J_2(2\omega)$ for C_1 appeared to be better through out the nematic range. These preliminary results are summarized in table V. The site dependences of spectral densities at two different temperatures (311 and 343K) are shown in figure 5.

TABLE V: Model parameters for 6OCB derived from Nordio's model. The diffusion constants and jump rates are in units of 10^9 s^{-1}.

T (K)	$D_\perp$	$D_\parallel$	D_R	k_1	k_2	k_3	Q (%)
311	0.05	0.49	1.4	2.1 x 10^2	5.3 x 10^5	1.2 x 10^8	1.0
335	0.04	1.38	3.9	2.5 x 10^2	2.1 x 10^6	3.9 x 10^7	2.7
343	0.05	2.37	4.7	2.1 x 10^2	5.3 x 10^5	1.1 x 10^8	2.4

SUMMARY AND CONCLUSIONS

We have successfully modeled the spectral densities of several nematogens of different chain lengths using the decoupled model that describes correlated internal motions. Using interaction parameters derived from modeling the segmental order parameter profile of the same deuterons, we found that both Nordio's and the third rate model could satisfactorily model the experimental spectral densities of 5CB. The error, calculated spectral densities and derived motional parameters were very similar for both models, so that for 5CB it is difficult to distinguish between the two models of molecular reorientation. This is not the case for 1O.4 whose reorientation motion can best be described by the third rate model. We have used Nordio's model for reorientation of 6OCB due to what we found in 5CB. Because of its longer chain length and the oxygen atom in the hexyloxy chain, we still could not fit the relaxation data of 6OCB over the entire nematic range as well as the other two nematogens. More accurate spectral density data may be required and the decoupled model may need further refinement. The jump rate k_1 for one-bond motion appears to be similar for all three nematogens as expected. Both the k_2

and k_3 tend to be larger as the chain length increases. The derived rotational diffusion constants for all the studied nematogens seem to have the same order of magnitude at the same reduced temperature (T/T_c). In conclusion, the decoupled model proposed by us appears to be useful to understand internal chain dynamics in several liquid crystals. A study of several members in a homoloque series can be valuable in revealing how the jump rates in the chain depend on its chain length.

ACKNOWLEDGMENTS

The financial support of the Natural Sciences and Engineering Council of Canada and the technical assistances of D. Bramadat and N. Finlay are gratefully acknowledged.

REFERENCES

1. P. A. Beckmann, J. W. Emsley, G. R. Luckhurst, and D.L. Turner, Mol. Phys., 50, 699 (1983); C. R. J. Counsell, J. W. Emsley, G. R. Luckhurst, D. L. Turner, and J. Charvolin, Mol. Phys., 52, 499 (1984).
2. P. A. Beckmann, J. W. Emsley, G. R. Luckhurst, and D. L. Turner,. Mol. Phys., 59, 97 (1986)
3. R. Y. Dong, Nuclear Magnetic Resonance of Liquid Crystals (Springer-Verlag, New York, 1994).
4. R. Y. Dong, Phys. Rev., 43, 4310 (1991); R. Y. Dong and G. M. Richards, Chem. Phys. Lett., 171, 389 (1990).
5. A. Ferrarini, G. J. Moro, and P. L. Nordio, Liq. Cryst., 8, 593 (1990).
6. R. J. Wittebort and A. Szabo, J. Chem. Phys., 69, 1722 (1978).
7. P. J. Flory, Statistical Mechanics of Chain Molecules (Interscience, New York, 1969).
8. R. Y. Dong and G. M. Richards, J. Chem. Soc. Faraday Trans., 88, 1885 (1992).
9. P. L. Nordio and P. Busolin, J. Chem. Phys., 55, 5485 (1971).
10. P. L. Nordio, G. Rigatti, and U. Segre, J. Chem. Phys., 56, 2117 (1972); Mol. Phys., 25, 129 (1973).
11. J. W. Emsley, G. R. Luckhurst, and C. P. Stockley, Proc. R. Soc. London, Ser. A, 381, 117 (1982).
12. E. T. Samulski and R. Y. Dong, J. Chem. Phys., 77, 5090 (1982).
13. R. Y. Dong, L. Friesen, and G. M. Richards, Mol. Phys., 81, 1017 (1994).
14. R. Y. Dong and G. Ravindranath, Liq. Cryst. (in press).
15. R. R. Vold and R. L. Vold, J. Chem. Phys., 88, 1443 (1988).
16. R. Y. Dong and X. Shen, Phys. Rev. E, 49, 538 (1994).

17. P. G. de Gennes, The Physics of Liquid Crystals (Clarendon, Oxford, 1974); P. Pincus, Solid State Commun., 7, 415 (1969).
18. R. Köllner, K. H. Schweikert, and F. Noack, Liq. Cryst., 13, 483 (1993).
19. W. H. Press, B. P. Flannery, S. A. Tenkolsky, and W. T. Vetterling, Numerical Recipes (Cambridge University, Cambridge, U.K., 1986).
20. R. Y. Dong and G. M. Richards, J. Chem. Soc. Faraday Trans., 84, 1053 (1988).
21. C. J. R. Counsell, J. W. Emsley, N. J. Heaton, and G. R. Luckhurst, Mol. Phys., 54, 847 (1985).
22. C. J. R. Counsell, J. W. Emsley, G. R. Luckhurst, and H. S. Sachdev, Mol. Phys., 63, 33 (1988).
23. B. R. Ratna and R. Shashidhar, Mol. Cryst. Liq. Cryst., 42, 185 (1977).